INTERNODES for Elliptic Problems

Paola Gervasio and Alfio Quarteroni

1 Introduction

The INTERNODES (INTERpolation for NOnconforming DEcompositionS) method is an interpolation based approach to solve partial differential equations by means of non-overlapping domain decomposition methods featuring non-conforming discretizations at the interfaces [3, 4]. The non-conformity at a given interface is induced by independent discretizations (as, e.g., h-fem or hp-fem) on two adjacent subdomains.

For second order elliptic problems, the well known mortar method uses a single L^2-projection operator *per* interface to match the non-conforming local solutions. INTERNODES instead employs two interpolation operators: the first one is used to enforce the continuity of the traces, the second one to enforce the conservation of fluxes across the interface.

In this paper we sketch the formulation of INTERNODES when it is applied to second-order elliptic problems on two-domains decompositions. Then we apply it to two test problems: the Kellogg's problem with piece-wise constant diffusion coefficients, and a problem featuring an infinitely differentiable solution. In both cases, the numerical results show that INTERNODES attains optimal rate of

P. Gervasio (✉)
DICATAM, Università degli Studi di Brescia, Brescia, Italy
e-mail: paola.gervasio@unibs.it

A. Quarteroni (✉)
MOX, Department of Mathematics, Politecnico di Milano, Milano, Italy

Institute of Mathematics, École Polytechnique Fédérale de Lausanne (EPFL), Lausanne, Switzerland
e-mail: alfio.quarteroni@polimi.it

convergence (i.e., that of the best approximation error in each subdomain), as predicted by the theoretical estimate proved in [4].

Let $\Omega \subset \mathbb{R}^d$, with $d = 2, 3$, be an open domain with Lipschitz boundary $\partial\Omega$, Ω_1 and Ω_2 be two non-overlapping subdomains with Lipschitz boundary such that $\overline{\Omega} = \overline{\Omega_1 \cup \Omega_2}$, and $\Gamma = \partial\Omega_1 \cap \partial\Omega_2$ be their common interface.

Given $\alpha \in L^\infty(\Omega)$, $\mathbf{b} \in W^{1,\infty}(\Omega)$, $\gamma \in L^\infty(\Omega)$, and $f \in H^{-1}(\Omega)$, we look for u_1 in Ω_1 and u_2 in Ω_2 such that

$$
\begin{cases}
-\nabla \cdot (\alpha_k \nabla u_k) + \mathbf{b} \cdot \nabla u_k + \gamma u_k = f & \text{in } \Omega_k, \quad k = 1, 2 \\
u_2 = u_1 & \text{on } \Gamma \\
\alpha_1 \frac{\partial u_1}{\partial \mathbf{n}_1} + \alpha_2 \frac{\partial u_2}{\partial \mathbf{n}_2} = 0 & \text{on } \Gamma \\
\text{boundary conditions} & \text{on } \partial\Omega,
\end{cases}
\tag{1}
$$

where $\mathbf{n}_k$ is the outward unit normal vector to $\partial\Omega_k$ and $\alpha_k = \alpha|_{\Omega_k}$. The transmission condition $(1)_2$ expresses the continuity of the solution across Γ, while $(1)_3$ enforces the conservation of normal fluxes across the interface, see [7].

2 Intergrid Operators for Non-conforming Discretization

We consider two a-priori *independent families of triangulations*: $\mathcal{T}_{1,h_1}$ in Ω_1 and $\mathcal{T}_{2,h_2}$ in Ω_2, respectively. The meshes in Ω_1 and in Ω_2 can be non-conforming on Γ and characterized by different mesh-sizes h_1 and h_2. Moreover, different polynomial degrees p_1 and p_2 can be used to define the finite element spaces. Inside each subdomain Ω_k we assume that the triangulations $\mathcal{T}_{k,h_k}$ are affine, regular and quasi-uniform [6, Ch. 3].

For $k = 1, 2$, let $X_{k,h_k} = \{v \in C^0(\overline{\Omega_k}) : v_{|T} \in \mathbb{P}_{p_k}, \forall T \in \mathcal{T}_{k,h_k}\}$ be the usual Lagrangian finite element spaces associated with $\mathcal{T}_{k,h_h}$, while $Y_{k,h_k} = \{\lambda = v|_\Gamma, v \in X_{k,h_k}\}$ are the spaces of traces on Γ of functions in X_{k,h_k}, whose dimension is n_k.

We denote by Γ_1 and Γ_2 the internal boundaries of Ω_1 and Ω_2, respectively, induced by the triangulations $\mathcal{T}_{1,h_1}$ and $\mathcal{T}_{2,h_2}$. If Γ is a straight segment, then $\Gamma_1 = \Gamma_2 = \Gamma$, otherwise Γ_1 and Γ_2 can be different (see Fig. 1).
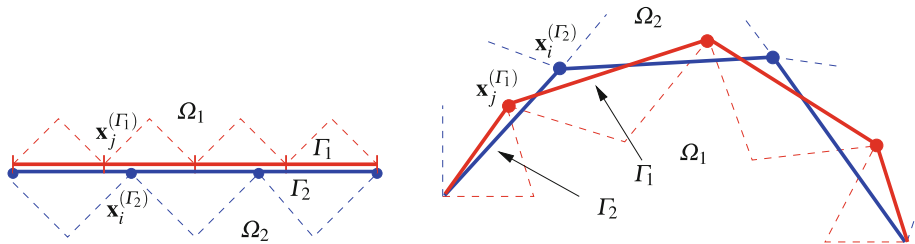
Fig. 1 Γ_1 and Γ_2 induced by the triangulations $\mathcal{T}_{1,h_1}$ and $\mathcal{T}_{2,h_2}$

For $k = 1, 2$, let $\{\mathbf{x}_1^{(\Gamma_k)}, \ldots, \mathbf{x}_{n_k}^{(\Gamma_k)}\} \in \overline{\Gamma}_k$ be the nodes induced by the mesh $\mathscr{T}_{k,h_k}$.

We introduce two independent operators that exchange information between the two independent grids on the interface Γ: $\Pi_{12} : Y_{2,h_2} \to Y_{1,h_1}$ and $\Pi_{21} : Y_{1,h_1} \to Y_{2,h_2}$.

If $\Gamma_1 = \Gamma_2$, Π_{12} and Π_{21} are the classical Lagrange interpolation operators defined by the relations:

$$(\Pi_{12}\mu_{2,h_2})(\mathbf{x}_i^{(\Gamma_1)}) = \mu_{2,h_2}(\mathbf{x}_i^{(\Gamma_1)}), \quad i = 1, \ldots, n_1, \qquad \forall \mu_{2,h_2} \in Y_{2,h_2}, \quad (2)$$

$$(\Pi_{21}\mu_{1,h_1})(\mathbf{x}_i^{(\Gamma_2)}) = \mu_{1,h_1}(\mathbf{x}_i^{(\Gamma_2)}), \quad i = 1, \ldots, n_2, \qquad \forall \mu_{1,h_1} \in Y_{1,h_1}. \quad (3)$$

If, instead, Γ_1 and Γ_2 are geometrical non-conforming, we define Π_{12} and Π_{21} as the Rescaled Localized Radial Basis Function (RL-RBF) interpolation operators introduced in formula (3.1) of [2]. More precisely, for $i = 1, \ldots, n_k$ let $\tilde{\phi}_i^{(k)}(\mathbf{x}) = \phi(\|\mathbf{x} - \mathbf{x}_i^{(\Gamma_k)}\|, r) = \max\{0, (1 - \|\mathbf{x} - \mathbf{x}_i^{(\Gamma_k)}\|/r)^4\}(1 + 4\|\mathbf{x} - \mathbf{x}_i^{(\Gamma_k)}\|/r)$ be the locally supported C^2 Wendland radial basis function [8] centered at $\mathbf{x}_i^{(\Gamma_k)}$ with radius $r > 0$. For any continuous function f on Ω, for $i = 1, \ldots, n_k$ let $(\gamma_f^{(k)})_i \in \mathbb{R}$ be the solutions of the system

$$\sum_{i=1}^{n_k}(\gamma_f^{(k)})_i\tilde{\phi}_i^{(k)}(\mathbf{x}_j^{(\Gamma_k)}) = f(\mathbf{x}_j^{(\Gamma_k)}), \qquad j = 1, \ldots, n_k$$

and set

$$(\Pi_{RBF}^{(k)}f)(\mathbf{x}) = \sum_{i=1}^{n_k}(\gamma_f^{(k)})_i\tilde{\phi}_i^{(k)}(\mathbf{x}).$$

Then, after setting $g(x) \equiv 1$, for any $\mu_{2,h_2} \in Y_{2,h_2}$ and $\mu_{1,h_1} \in Y_{1,h_1}$, the RL-RBF interpolation operators are defined by

$$(\Pi_{12}\mu_{2,h_2})(\mathbf{x}) = \frac{(\Pi_{RBF}^{(2)}\mu_{2,h_2})(\mathbf{x})}{(\Pi_{RBF}^{(2)}g)(\mathbf{x})}, \qquad (\Pi_{21}\mu_{1,h_1})(\mathbf{x}) = \frac{(\Pi_{RBF}^{(1)}\mu_{1,h_1})(\mathbf{x})}{(\Pi_{RBF}^{(1)}g)(\mathbf{x})}.$$

In both cases, the (rectangular) matrices associated with Π_{12} and Π_{21} are, respectively, $R_{12} \in \mathbb{R}^{n_1 \times n_2}$ and $R_{21} \in \mathbb{R}^{n_2 \times n_1}$ and they are defined by

$$\begin{aligned}(R_{12})_{ij} &= (\Pi_{12}\mu_j^{(2)})(\mathbf{x}_i^{(\Gamma_1)}) & i = 1, \ldots, n_1, \; j = 1, \ldots, n_2, \\(R_{21})_{ij} &= (\Pi_{21}\mu_j^{(1)})(\mathbf{x}_i^{(\Gamma_2)}) & i = 1, \ldots, n_2, \; j = 1, \ldots, n_1,\end{aligned} \qquad (4)$$

where $\{\mu_i^{(k)}\}$ are the Lagrange basis functions of Y_{k,h_k}, for $k = 1, 2$ and $i = 1, \ldots, n_k$.

Obviously, in the conforming case for which $\Gamma_1 = \Gamma_2$, $h_1 = h_2$ and $p_1 = p_2$, the interpolation operators Π_{12} and Π_{21} are the identity operator and $R_{12} = R_{21} = I$ (the identity matrix of size $n_1 = n_2$). Finally, let

$$(M_{\Gamma_k})_{ij} = (\mu_j^{(k)}, \mu_i^{(k)})_{L^2(\Gamma_k)}, \qquad k = 1, 2, \tag{5}$$

the *interface mass matrices*. We notice that only information associated with the interface nodes (more precisely, the nodes coordinates) are needed to assemble both the interface mass matrices and the interpolation matrices for both the Lagrange and the RL-RBF interpolation approaches.

3 Mathematical Foundation of INTERNODES for Elliptic Problems

Let us consider the transmission problem (1) and, for simplicity, we complete it with homogeneous Dirichlet boundary conditions on $\partial\Omega$. For $k = 1, 2$ we introduce the local spaces $V_k = \{v \in H^1(\Omega_k) \mid v = 0 \text{ on } \partial\Omega \cap \partial\Omega_k\}$, $V_k^0 = \{v \in V_k \mid v = 0 \text{ on } \Gamma\}$, the bilinear forms $a_k : V_k \times V_k \to \mathbb{R}$: $a_k(u, v) = \int_{\Omega_k} (\alpha_k \nabla u \cdot \nabla v + (\mathbf{b} \cdot \nabla u)v + \gamma uv)d\Omega$, and the finite dimensional spaces $V_{k,h_k} = X_{k,h_k} \cap V_k$, $V_{k,h_k}^0 = X_{k,h_k} \cap V_k^0$, and $\Lambda_{k,h_k} = \{\lambda = v|_\Gamma, \ v \in V_{k,h_k}\}$. Let $\mathscr{R}_k : \Lambda_{k,h_k} \to V_{k,h_k}$, s.t. $(\mathscr{R}_k\eta_{k,h_k})|_\Gamma = \eta_{k,h_k}$, $\forall \eta_{k,h_k} \in \Lambda_{k,h_k}$ be any linear and continuous discrete lifting from Γ_k to Ω_k (as, e.g., the finite element interpolant that is zero at all finite element nodes not lying on Γ_k). Finally, we denote by $\mathscr{I}_k$ the set of indices $i \in \{1, \ldots, n_k\}$ of the nodes $\mathbf{x}_i^{(\Gamma_k)}$ of Γ_k.

In order to apply the INTERNODES method to problem (1), for any $v_{k,h_k} \in V_{k,h_k}$ and for $k = 1, 2$ we define the scalar quantities

$$\begin{aligned}
(r_v^{(k)})_i &= a_k(v_{k,h_k}, \mathscr{R}_k\mu_i^{(k)}) - (f, \mathscr{R}_k\mu_i^{(k)})_{L^2(\Omega_k)}, & i \in \mathscr{I}_k, \\
(z_v^{(k)})_j &= \sum_{i \in \mathscr{I}_k} (M_{\Gamma_k}^{-1})_{ji}(r_v^{(k)})_i, & j \in \mathscr{I}_k,
\end{aligned} \tag{6}$$

and the functions

$$(r_v)_{k,h_k} = \sum_{j \in \mathscr{I}_k} (z_v^{(k)})_j \mu_j^{(k)}, \tag{7}$$

belonging to Λ_{k,h_k}. (The subscript v highlights the dependence of r on v.)

Remark 1 When non-homogeneous Dirichlet boundary conditions are assigned on $\partial\Omega$, we can recover the homogeneous case by a lifting of the Dirichlet data, so that only the right hand side has to be modified (see, e.g., [6]).

The weak form of INTERNODES applied to (1) reads: find $u_{1,h_1} \in V_{1,h_1}$ and $u_{2,h_2} \in V_{2,h_2}$ such that

$$
\begin{cases}
a_k(u_{k,h_k}, v_{k,h_k}) = (f, v_{k,h_k})_{L^2(\Omega_k)} \ \forall v_{k,h_k} \in V_{k,h_k}^0, & k = 1, 2 \\
u_{2,h_2} = \Pi_{21} u_{1,h_1} & \text{on } \Gamma_2, \\
(r_u)_{1,h_1} + \Pi_{12}(r_u)_{2,h_2} = 0 & \text{on } \Gamma_1.
\end{cases}
\tag{8}
$$

For $k = 1, 2$, $(r_u)_{k,h_k} \in Y_{k,h_k}$ are the so-called *residuals* at the interface Γ_k. In fact they are the discrete fluxes across the interface, i.e., they represent the approximations of $\alpha_k \partial u_k / \partial \mathbf{n}_k$ on Γ_k.

Remark 2 The values $(r_u^{(k)})_i$ are not the coefficients of $(r_u)_{k,h_k}$ w.r.t. the Lagrange basis $\{\mu_i^{(k)}\}$ (on which we can apply the interpolation). Rather, they are the coefficients of $(r_u)_{k,h_k}$ w.r.t. the dual basis $\{\psi_i^{(k)}\}_{i=1}^{n_k}$ of Y'_{k,h_k} defined by the relations $(\psi_i^{(k)}, \mu_j^{(k)})_{L^2(\Gamma_k)} = \delta_{ij}$, for $i, j = 1, \ldots, n_k$ (δ_{ij} is the Kronecker delta), precisely,

$$
(r_u)_{k,h_k} = \sum_{i \in \mathscr{I}_k} (r_u)_i^{(k)} \psi_i^{(k)}.
$$

Y_{k,h_k} and Y'_{k,h_k} are identical linear spaces and it can be proved that $\psi_i^{(k)} = \sum_{j \in \mathscr{I}_k} (M_{\Gamma_k}^{-1})_{ji} \mu_j^{(k)}$ for any $i \in \mathscr{I}_k$, therefore (7) follows. The interface mass matrix M_{Γ_k} and its inverse play the role of transfer matrices from the Lagrange basis to the dual one and vice versa, respectively.

Denoting by z_k and r_k the arrays whose entries are the values $(z_u^{(k)})_j$ and $(r_u^{(k)})_i$, respectively, it follows that $\mathsf{z}_k = M_{\Gamma_k}^{-1} \mathsf{r}_k$.

Then, the algebraic form of the interface condition (8)$_3$ reads

$$
M_{\Gamma_1}^{-1} \mathsf{r}_1 + R_{12} M_{\Gamma_2}^{-1} \mathsf{r}_2 = 0,
$$

or, equivalently, $\mathsf{r}_1 + M_{\Gamma_1} R_{12} M_{\Gamma_2}^{-1} \mathsf{r}_2 = 0$.

For $k = 1, 2$ let u_k denote the array of the Lagrange coefficients of u_{k,h_k} at the nodes of $\mathscr{T}_{k,h_k}$ and $\boldsymbol{\lambda}_k$ the array of the Lagrange coefficients of u_{k,h_k} at the nodes of $\mathscr{T}_{k,h_k} \cap \Gamma_k$. Denoting by A_k the finite element stiffness matrices associated with the discretization of (8)$_1$, the algebraic form of (8) reads:

$$
\begin{cases}
A_k \mathsf{u}_k = \mathsf{f}_k, & k = 1, 2, \\
\boldsymbol{\lambda}_2 = R_{21} \boldsymbol{\lambda}_1, & \\
\mathsf{r}_1 + M_{\Gamma_1} R_{12} M_{\Gamma_2}^{-1} \mathsf{r}_2 = 0,
\end{cases}
\tag{9}
$$

with $\mathsf{u}_{k|\Gamma_k} = \boldsymbol{\lambda}_k$.

Under the assumption that problem (1) is well posed (see, e.g., [4, 6]) the following convergence theorem, assessing the optimal error bound for the INTERNODES method, is proved in [4].

Theorem 1 *Assuming that $u \in H^s(\Omega)$, with $s > 3/2$, $\lambda = u_{|\Gamma} \in H^\sigma(\Gamma)$, with $\sigma > 1$, $(\alpha_k \partial u_2 / \partial \mathbf{n}_2) \in H^\nu(\Gamma)$, with $\nu > 0$, if $p_k \geq 1$ is the finite element polynomial degree in Ω_k, $k = 1, 2$, and Lagrange interpolation is used to define Π_{12} and Π_{21}, there exist $\frac{1}{2} \leq q < 1$ and $\frac{3}{2} \leq z < 2$ s.t.*

$$\|u - u_h\|_* \lesssim h_1^{\ell_1-1}\|u\|_{H^s(\Omega_1)} + h_2^{\ell_2-1}\|u\|_{H^s(\Omega_2)}$$
$$+ \left(h_1^{\varrho_1-1/2} + h_2^{\varrho_2-1/2} + h_1^{\varrho_1-1/2}\left(\frac{h_2}{h_1}\right)^q \right)\|\lambda\|_{H^\sigma(\Gamma)}$$
$$+ \left(h_1^{\zeta_1+1/2} + h_2^{\zeta_2+1/2} + h_1^{\zeta_1+1/2}\left(\frac{h_1}{h_2}\right)^z \right)\|r_2\|_{H^\nu(\Gamma)},$$

with $\ell_k = \min(s, p_k + 1)$, $\varrho_k = \min(\sigma, p_k + 1)$, $\zeta_k = \min(\nu, p_k + 1)$, and being $\|v\|_* = \{\|v\|_{H^1(\Omega_1)}^2 + \|v\|_{H^1(\Omega_2)}^2\}^{1/2}$ the broken norm on Ω.

Remark 3 Π_{21} is used to match the traces, while Π_{12} is used to match the residuals, i.e. the fluxes.

Using instead only one intergrid interpolation operator would not guarantee an accurate non-conforming method; for example using only Π_{21} yields to the so-called *point wise matching* discussed, e.g., in [1]. At the algebraic level the latter approach uses only the matrix R_{21} and its transpose R_{21}^T, whereas INTERNODES uses both R_{21} and R_{12}.

Remark 4 (On the Conservation of Fluxes) The conservation of fluxes across the interface at the discrete level is enforced by the interface condition $(8)_3$. As this property depends on the interpolation operator Π_{12}, that in turns depends on the choice of the local subspaces, the flux jump vanishes, as h_1 and h_2 go to zero, with the same order of the broken norm of the error.

Remark 5 The INTERNODES method can be generalized to decompositions with more than two subdomains, possibly featuring internal cross-points (i.e., points shared almost among three subdomains). We refer to [4, Sect. 6] for a detailed description of the algorithm. What follows is a sketch of the generalization of INTERNODES when $\Omega \subset \mathbb{R}^2$. Let Ω_k and Ω_ℓ be two generic subdomains such that $\Gamma_{k\ell} = \partial \Omega_k \cap \partial \Omega_\ell$ is neither empty nor reduced to a vertex, while $\gamma_k^{(i)}$ and $\gamma_\ell^{(j)}$ denote the edges of $\partial \Omega_k$ and $\partial \Omega_\ell$, respectively, such that $\Gamma_{k\ell} = \gamma_k^{(i)} \cap \gamma_\ell^{(j)}$.

Two typical situations can occur: the end-points of $\gamma_k^{(i)}$ coincide with those of $\gamma_\ell^{(j)}$ (as in Fig. 2), or not (as in Fig. 3). In the first case, each interface $\Gamma_{k\ell}$ is handled as in the case of only two subdomains and we build couples of intergrid matrices $R_{\ell k}$ and $R_{k\ell}$ from $\gamma_k^{(i)}$ to $\gamma_\ell^{(j)}$ and vice versa, as done in Sect. 2. In the second case, let us suppose that the measure of $\gamma_k^{(i)}$ is larger than that of $\gamma_\ell^{(j)}$. Here all the
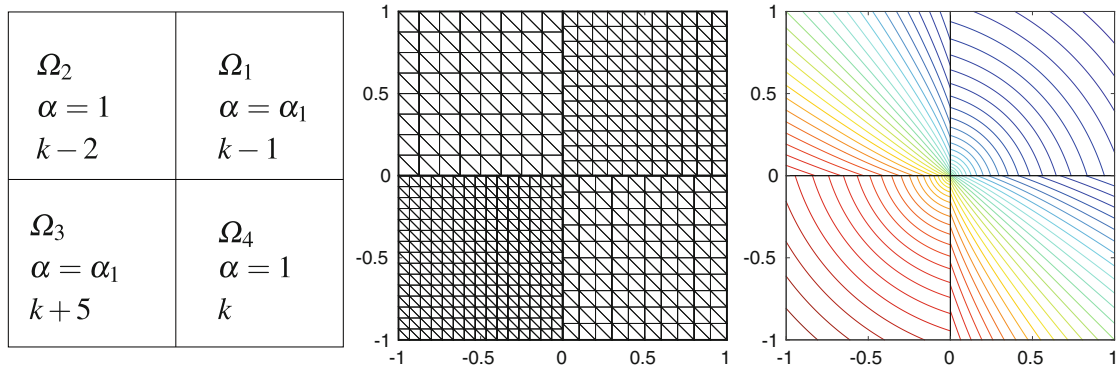
Fig. 2 At left, the decomposition of Ω into four subdomains. In the middle, the nonconforming $\mathbb{P}_1$ meshes for $k = 10$. At right, the Kellogg's solution with $\gamma = 0.4$ and $\alpha_1 = 9.472135954999585$ computed by INTERNODES and $\mathbb{P}_1$
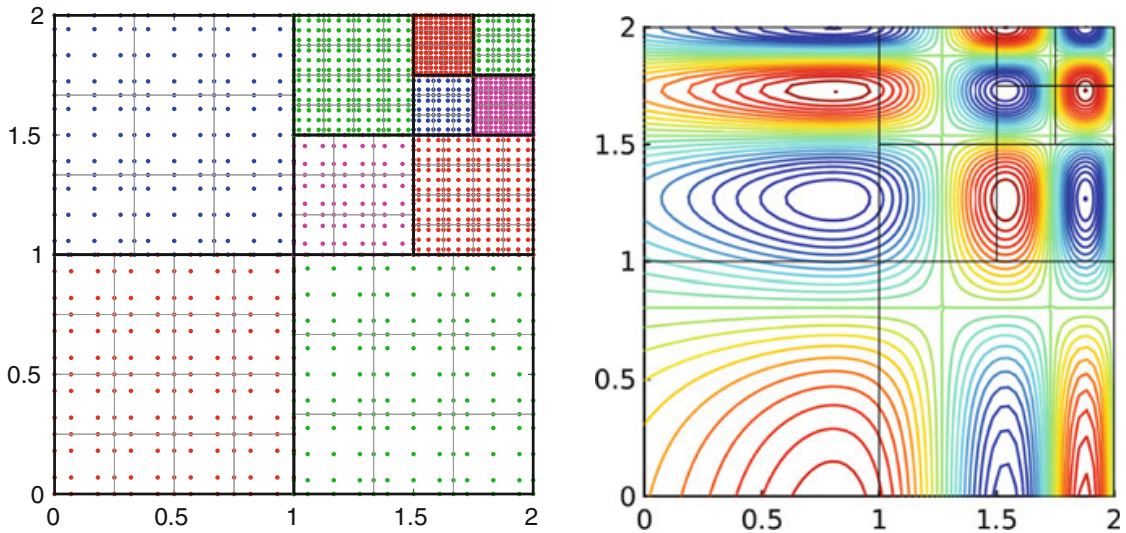
Fig. 3 At left, a partition of the computational domain into 10 subdomains; in each subdomain the quad *hp*-fem mesh is plotted, different colours refer to different subdomains. At right, the corresponding INTERNODES solution

basis functions living on $\gamma_k^{(i)}$ whose support has non-empty intersection with $\gamma_\ell^{(j)}$ must be taken into account when building the interpolation matrices $R_{\ell k}$ and $R_{k\ell}$ and the interface mass matrices $M_{\ell k}$ and $M_{k\ell}$. Alternatively, one can build both the interface mass matrices and the interpolation matrices on the larger interface $\gamma_k^{(i)}$ by assembling the contributions arising from all the shorter edges of the subdomains adjacent to Ω_k on the other side of $\gamma_k^{(i)}$.

Remark 6 Robin conditions could be used instead of Neumann ones. The formulation of INTERNODES would not change, provided the interface conditions are imposed weakly (as *natural* conditions). As a matter of fact, natural interface conditions are automatically accounted for when evaluating the discrete residuals of the differential problem as done in (6).

4 Numerical Results: The Kellogg's Test Case

We test INTERNODES on a very challenging problem whose solution features low regularity. The so-called Kellogg's function (see, e.g., [5]) is an exact weak solution of the elliptic problem

$$
\begin{cases}
-\nabla \cdot (\alpha \nabla u) = 0 & \text{in } \Omega = (-1, 1)^2 \\
\text{Dirichlet boundary conditions} & \text{on } \partial \Omega,
\end{cases}
\tag{10}
$$

with piece-wise constant coefficient α: $\alpha = \alpha_1 > 0$ in the first and the third quadrants, and $\alpha = 1$ in the second and in the fourth ones. It can be written in terms of the polar coordinates r and θ as $u(r, \theta) = r^\gamma \mu(\theta)$, where $\gamma \in (0, 2)$ is a given parameter, while $\mu(\theta)$ is a $2\pi-$periodic continuous function (more regular only when $\gamma = 1$). The case $\gamma = 1$ is trivial since the solution is a plane. The positive value α_1 depends on γ and on two other real parameters σ and ρ. The set $\{\alpha_1, \gamma, \sigma, \rho\}$ must satisfy a nonlinear system (see formula (5.1) of [5]). In particular we fixed $\rho = \pi/4$.

When $\gamma \neq 1$, $u \in H^{1+\gamma-\varepsilon}(\Omega)$, for any $\varepsilon > 0$; the solution features low regularity at the origin and its normal derivatives to the axis are discontinuous.

We solve problem (10) by applying INTERNODES to the 4-subdomains decomposition induced by the discontinuity of α and by using either $\mathbb{P}_1$ or $\mathbb{Q}_2$ finite elements in each subdomain (see the $\mathbb{P}_1$ mesh in Fig. 2). The meshes at the interfaces are non-conforming as shown in Fig. 2, more precisely given $k \in \mathbb{N}$, the subdomains mesh-sizes are: $h_1 = 1/(k - 1)$, $h_2 = 1/(k - 2)$, $h_3 = 1/(k + 5)$ and $h_4 = 1/k$.

By refining the meshes (we cycle on $k = 20, 40, 80, 160$), we measure the convergence order of INTERNODES on the Kellogg's solution for different values of the parameter γ. The results are shown in Table 1 and the convergence estimate provided by Theorem 1 for two subdomains is here confirmed, although this test case involves four subdomains instead of two.

We highlight that, although INTERNODES is based on interpolation operators rather than projections (as in the mortar methods), the best approximation error of the finite element discretization is preserved and not downgraded.

Table 1 Convergence orders of INTERNODES for the Kellogg's test solution

γ	s	σ	ν	$\min\{\ell - 1, \rho - 1/2, \zeta + 1/2\}$	$\mathbb{P}_1$ order	$\mathbb{Q}_2$ order
0.4	$1.4 - \varepsilon$	$0.9 - \varepsilon$	$0.4 - \varepsilon$	$0.4 - \varepsilon$	0.363	0.429
0.6	$1.6 - \varepsilon$	$1.1 - \varepsilon$	$0.6 - \varepsilon$	$0.6 - \varepsilon$	0.574	0.651
1.4	$2.4 - \varepsilon$	$1.9 - \varepsilon$	$1.4 - \varepsilon$	1 for $\mathbb{P}_1$, $1.4 - \varepsilon$ for $\mathbb{Q}_2$	0.955	1.394
1.8	$2.8 - \varepsilon$	$2.3 - \varepsilon$	$1.8 - \varepsilon$	1 for $\mathbb{P}_1$, $1.8 - \varepsilon$ for $\mathbb{Q}_2$	0.949	1.615

The case $\gamma = 0.4$ is not covered by the convergence Theorem 1 since $s < 3/2$ and $\sigma < 1$. $\min\{\ell - 1, \rho - 1/2, \zeta + 1/2\}$ is the expected convergence order provided by Theorem 1, the measured convergence orders are shown in the last two columns

## 5   Numerical Results: Infinite Differentiable Solution

Let us consider the problem (1) with $\alpha = 1$, $\mathbf{b} = [1, 1]$, $\gamma = 1$ on $\Omega = (0, 2)^2$. The boundary data and the function f are such that the exact solution is $u(x, y) = \sin(3\pi \exp(3(x - 2)/2)) \cos(3\pi \exp(3(y - 2)/2))$.

A decomposition of $\Omega = (0, 2)^2$ in 10 subdomains as in Fig. 3 is considered, and independent triangulations in each Ω_k are designed so that on each interface both polynomial non-conformity and geometric non-conformity may occur. Either $\mathbb{P}_1$ and quadrilateral hp-fem ($\mathbb{Q}_p$) are used to approximate the numerical solution. A non-conforming grid, obtained with $\mathbb{Q}_p$ discretizations in each subdomain, is shown in Fig. 3, left. In order to guarantee full non-conformity on each interface, we have set on two adjacent domains the polynomial degree equal to either $p = 3$ or $p = 4$ and the local mesh size equal to either $h = 1/4$ or $h = 1/3$. In Fig. 3, right, the corresponding numerical solution computed by INTERNODES is shown.

In order to measure the errors in broken norm, we take the same polynomial degree p in each subdomain and we consider only geometric non-conformity as in Fig. 3, left, but with a variable number k (or $k - 1$) of elements (more precisely, $k = 4$ in Fig. 3, left). The reference parameter is the mesh size $h = 1/k$ of the left-bottom subdomain. In Fig. 4, the errors in broken norm are reported, w.r.t. to both h and p.

The error behaviour versus h (see Fig. 4 left) agrees with the theoretical estimate of Theorem 1, for which we expect $\|u - u_h\|_* \le c(u)h^p$ (in this case $p = 1, 2, 4$), as u is infinitely differentiable.

The convergence rate vs p shown in Fig. 4, right, is more than algebraic, as typical in hp-fem.
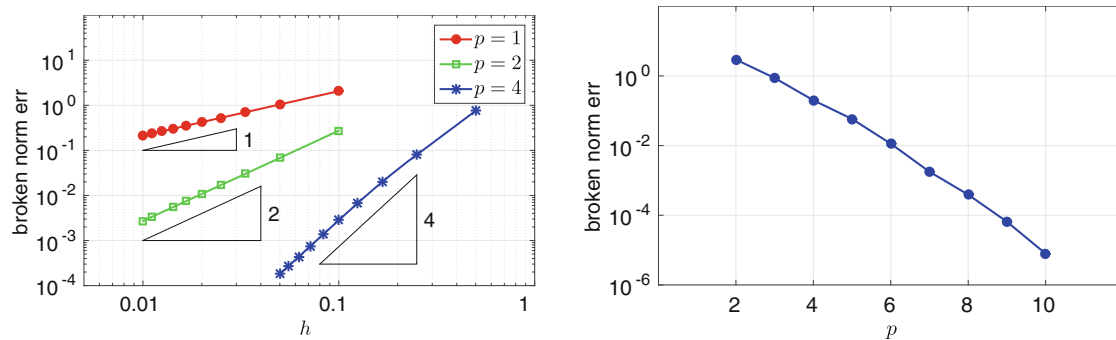
Fig. 4 At left, the broken norm error w.r.t. the mesh-size h of the bottom-left subdomain, p is fixed. At right, the broken norm error w.r.t. p, here the meshes sizes are fixed: that of the left-bottom subdomain is $h = 1/4$

References

1. C. Bernardi, Y. Maday, A.T. Patera, A new nonconforming approach to domain decomposition: the mortar element method, in *Nonlinear Partial Differential Equations and Their Applications. Collège de France Seminar, Vol. XI* (Paris, 1989–1991). Pitman Research Notes in Mathematics Series, vol. 299 (Longman Scientific and Technical, Harlow, 1994), pp. 13–51
2. S. Deparis, D. Forti, A. Quarteroni, A rescaled localized radial basis function interpolation on non-Cartesian and nonconforming grids. SIAM J. Sci. Comput. **36**(6), A2745–A2762 (2014)
3. S. Deparis, D. Forti, P. Gervasio, A. Quarteroni, INTERNODES: an accurate interpolation-based method for coupling the Galerkin solutions of PDEs on subdomains featuring non-conforming interfaces. Comput. Fluids **141**, 22–41 (2016)
4. P. Gervasio, A. Quarteroni, Analysis of the INTERNODES method for non-conforming discretizations of elliptic equations. Comput. Methods Appl. Mech. Eng. **334**, 138–166 (2018). https://doi.org/10.1016/j.cma.2018.02.004
5. P. Morin, R.H. Nochetto, K.G. Siebert, Data oscillation and convergence of adaptive FEM. SIAM J. Numer. Anal. **38**(2), 466–488 (2000)
6. A. Quarteroni, A. Valli, *Numerical Approximation of Partial Differential Equations* (Springer, Heidelberg, 1994)
7. A. Quarteroni, A. Valli, *Domain Decomposition Methods for Partial Differential Equations* (Oxford University Press, Oxford, 1999)
8. H. Wendland, Piecewise polynomial, positive definite and compactly supported radial functions of minimal degree. Adv. Comput. Math. **4**(1), 389–396 (1995)